Presented at the 29th European PV Solar Energy Conference and Exhibition, 22-26 September 2014, Amsterdam, The Netherlands

LOCAL BORON DOPING FOR P-TYPE PERL SILICON SOLAR CELLS FABRICATED BY LASER PROCESSING OF DOPED SILICON NANOPARTICLE PASTE

U. Jäger[1], A. Wolf[1], C. Wufka[1], Y. Tomizawa[2], T. Imamura[2], M. Soeda[2,3], Y. Ikeda[2], T. Shiro[2,3]

[1]Fraunhofer Institute for Solar Energy Systems (ISE), Heidenhofstraße 2, D-79110 Freiburg, Germany
[2]Electronics Materials Development Project, New Business Development Business Unit, Teijin Limited, 4-3-2, Asahigaoka, Hino-shi, Tokyo 191-8512, Japan
[3]NanoGram Corporation, 165 Topaz Street, Milpitas, CA 95035, USA
Corresponding author: Ulrich Jäger, email: ulrich.jaeger@ise.fraunhofer.de, Phone: +49 761 4588 5057

ABSTRACT: We present the fabrication of local boron doping for local contacts for p-type PERL solar cells. A boron doped silicon nanoparticle paste is printed onto the passivated rear side of the wafer and is locally diffused into the wafer by an adapted laser process. Thus a local p+ doping is formed and the passivation is opened in a single processing step. After a description of the process and the properties of the local boron doping, fabricated solar cells are discussed. A maximum conversion efficiency of 20.0% is achieved for PERL type solar cells on 6-inch MCz-Si wafers. High fill factors above 79% and high open circuit voltages above 650 mV are observed, highlighting the effectiveness of the local back surface field underneath the rear side point contacts.
Keywords: laser processing, passivated silicon solar cell, boron doping

1 INTRODUCTION

Solar cell research aims at lowering the fabrications costs per watt peak. Advanced cell concepts, such as passivated emitter and rear cells (PERC) and passivated emitter and rear locally diffused (PERL) cells allow the suppression of optical and recombinative losses [1, 2] at the cell's rear surface. However, for such devices local contacts have to be fabricated at the rear side of the cell. Furthermore, locally highly doped point contacts are beneficial for such cells, as both recombination (by field effect passivation) and resistive losses (by a low metal-semiconductor resistance) are suppressed. This local doping is commonly referred to as a local back surface field (LBSF). Several approaches have been proposed to fabricate local doping at the rear side of p-type PERC/PERL cells: the laser fire contacts (LFC) approach drives the Al through the rear side passivation layer using a laser after contact firing and forming a local BSF and contact [3]. The other common approach is to locally open the passivation (using a laser or an etching paste) and print Al on top and create a local BSF during fast firing [4]. Both approaches have been implemented into pilot line production [5, 6]. However, in either case the LBSF consists of Al. Boron can provide a better BSF as it can be incorporated into the silicon at higher concentrations than Al.

In this paper, we propose the fabrication of a local boron back surface field by applying an adapted laser process to a screen printed boron doped silicon nanoparticle paste on the passivated rear side [7] of cell precursors. This process creates a local doping as well as an opening in the passivating layer. The rear side electrode consists of evaporated aluminum (Al).

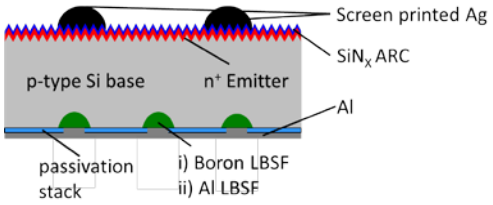

Figure 1: Cross section of PERC/PERL cells. In case i) the local back surface field consists of boron and in ii) of aluminum. The rear side electrode (Al) is either evaporated or screen printed. See section 2.4 for details of cell fabrication.

2 SAMPLE PREPARATION

Several samples were prepared to investigate the properties of the laser induced boron doping. If not mentioned elsewise, the silicon nanoparticle paste containing boron (NanoGram® Boron doped Si paste) from NanoGram Corp. was applied by a conventional screen printing tool. Drying of the printed paste was done under similar conditions as for a conventional metal paste. Removal of the paste after laser processing was done in diluted KOH for 60 s.

2.1 Laser Doping

To investigate the resulting boron doping after laser processing samples were prepared as described in the following (see figure 2a). n-type Cz-Si wafers were damage etched and on a single side a passivating stack of AlO_X/SiN_X was deposited by plasma enhanced chemical vapor deposition (PECVD) to simulate the conditions at the rear side of the cell. Subsequently the doped nano-particle paste was applied, dried and a solid state disc laser at f_{rep} = 30 kHz (λ = 1030 nm) was used to create local p+ doping. To allow for an easy characterization of the fabricated pn-structure, fields of full area laser doping of 20x20 mm² were processed. After washing off the remaining paste the samples were investigated for their resulting sheet resistance R_{sheet} by 4 point probing (4pp) and the doping profiles was measured by electrochemical capacitance voltage (ECV).

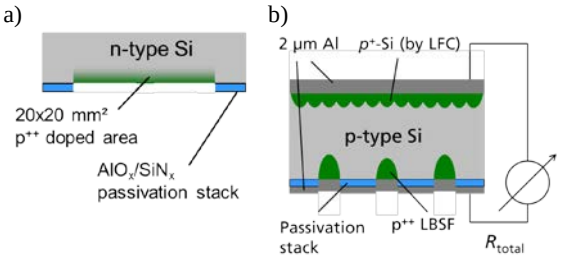

Figure 2: Schematic of the samples for investigation of a) doping properties and b) contact resistance. The samples are described in detail in the text.

2.2 Semiconductor-metal contact properties

To investigate the properties of the metal semiconductor contact, special samples were prepared (see figure 2b). p-type Cz-Si wafers with a base resistivity of $\rho = 2.1\ \Omega$cm and an initial wafer thickness of $W = 200$ µm were damage etched and on the rear side a passivating stack of AlO_X/SiN_X was deposited by PECVD. On top of that stack the doped silicon nanoparticle paste was printed and dried. A fixed number of 100 point contacts were fabricated using the laser described in section 2.1. Then the remaining paste was washed off and 2 µm of Al were deposited by evaporation. On the front side of the samples a full area contact was formed using the LFC approach [3], ensuring a good ohmic contact over a large area. The samples were then annealed at 350 °C for 120 s. After that the wafers were cleaved into individual small samples and the resulting resistance from front to rear was measured using a multimeter.

2.3 Recombination at point contact

The recombination properties of the local doping was investigated based on a method proposed by Fischer [8] and is further discussed in section 3.3. The sample structure is shown in figure 3. High lifetime p-type float zone Si wafers with a base resistivity of $\rho = 2\ \Omega$cm and an initial wafer thickness of $W = 200$ µm were damaged etched and both front and rear side were coated with a passivating stack of AlO_X/SiN_X. After being submitted to a fast firing step to activate passivation (and simulate contact firing) the rear side of the samples was coated with the screen printed boron doped silicon nanoparticle paste. Point contacts with different contact pitches L_P were created by laser processing with the laser system described above in section 2.1. After washing off the remaining paste the samples' effective minority carrier lifetime was measured by quasi steady state photoconductance (QSSPC) before and after a short forming gas annealing step (350 °C, 120 s). The authors note that the unpassivated, open point contacts are assumed to have a similar surface recombination as a metallized surface.

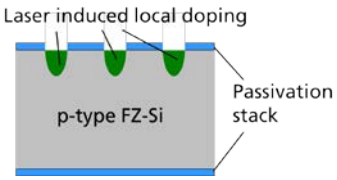

Figure 3: Schematic of the sample fabricated for evaluation of the recombination at the point contact.

2.4 Solar cells

To demonstrate the applicability of the developed process, PERL/PERC solar cells were fabricated with both evaporated Al and screen printed Al rear side electrodes. Magnetic Cz-Si with a base resistivity of 1.3 Ωcm, an area of $A = 238$ cm² and an initial thickness of $W = 200$ µm was used. The process flow is shown in Figure 4.

After damage etching a rear side masking layer was applied, serving both as a masking layer against texturing and as a diffusion barrier. The wafers were diffused in a tube furnace in a $POCl_3$ atmosphere and in a subsequent PSG etch the PSG and the rear side masking layer was etched off. The rear side was coated with an AlO_X/SiN_X passivation layer stack deposited by PECVD. The front side received an anti-reflective coating of PECVD SiN_X. For groups 1 and 2, an Ag front side electrode was applied by screen printing and these wafers were submitted to a fast firing step. After that, boron containing silicon nanoparticle paste from NanoGram Corp. was applied to the rear side of samples of groups 2 by means of screen printing. Local boron doping was done in a point contact pattern by a laser process as described in section 2. The remaining doped paste was washed off in diluted KOH. Wafers in groups 1 and 3 received local contact opening by applying screen printed etching paste, creating line openings. Subsequently, the rear side of groups 1 and 2 was coated with 2 µm of evaporated Al and wafers of group 3 received screen printed Al electrodes on the rear side and an Ag grid on the front side. Group 3 was then submitted to a fast firing step. Cells of groups 1 and 2 received a short forming gas (350 °C, 120 sec) anneal before all cells were measured for their *J-V* characteristics.

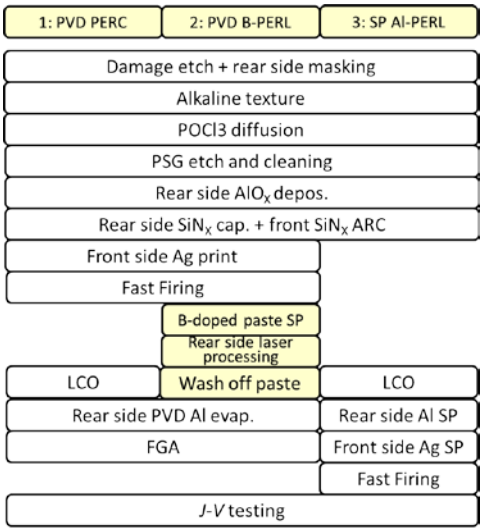

Figure 4: Process flow for PERC/PERL solar cells of groups 1-3. The groups are divided into physical vapor deposition (PVD) of rear side Al and screen printed (SP) Al as well as into group featuring a mere local contact opening (LCO).

3 EXPERIMENTAL RESULTS AND DISCUSSION

3.1 Sheet resistance and doping profiles

Figure 5 shows the resulting sheet resistance after boron laser doping onto the n-Si substrate. The sheet

resistance can be lowered by increasing laser power P. At values $P > 24$ W the silicon is being ablated therefore any increase in laser power leads to unwanted removal of material. Values as low as $R_{sheet} = 26\ \Omega$/sq are achieved after laser processing.

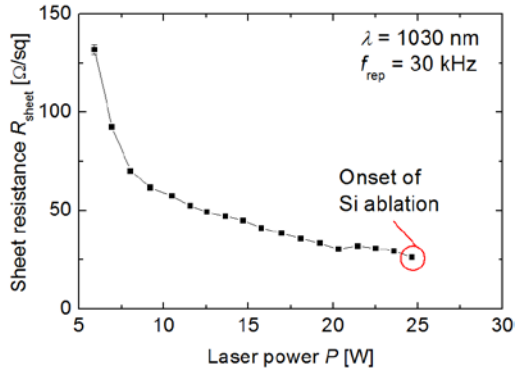

Figure 5: Evolution of the sheet resistance with increased laser power. The onset of silicon ablation is shown in the graph.

Figure 6 shows three measured doping profiles acquired by ECV. As the laser power is increased, the boron profile is driven deeper into the silicon and the surface concentration is lowered. Thus, the doping profile can be tailored by adapting the laser power.

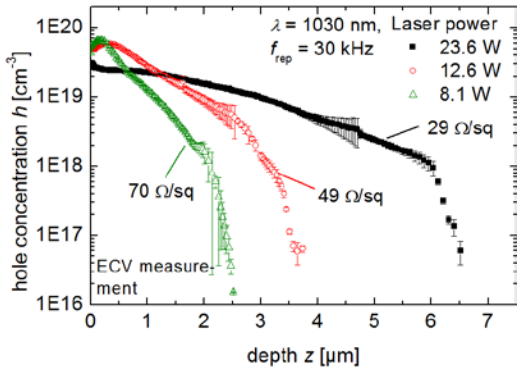

Figure 6: Doping profiles measured by ECV. If a single ionization of the boron atoms is assumed these doping profiles correspond to the boron doping in the silicon. The corresponding value of R_{sheet} is indicated.

3.2 Local contact properties

To give proof of the formation of an ohmic contact with a sufficiently low transition resistance, i.e. contact resistance the resistance per individual point contact was measured and evaluated. To allow for a sound comparison the so called spreading resistance R_{spread}

$$R_{spread} = \frac{\rho}{2\pi r_c}\arctan\left(\frac{2W}{r_c}\right) \qquad (1)$$

as proposed by Cox and Strack [9] was calculated for each individual laser parameter: the contact area was measured by light microscope (contact diameter $2r_c$) and the wafers' individual base doping (ρ in Ωcm) and thickness W were determined prior to processing for this kind of samples. This comparison is shown in Figure 7. It is observed that for all investigated laser parameters the determined contact resistance is lower than the value for the spreading resistance (as much as 55% below the value of the corresponding spreading resistance R_{spread}). This can be explained by the additional boron doping that is present at the point contacts and it is assumed that therefore detrimental effects of current crowding become less prominent.

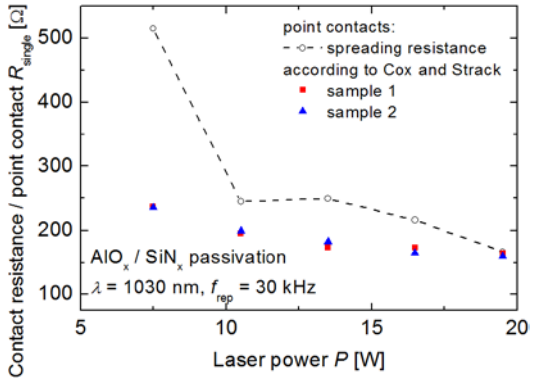

Figure 7: Comparison between measured contact resistance per single contact R_{single} for two identical processed samples and the limit given by the parameterization of Cox and Strack for a point contact. The observed values are as much as 55% lower than the theoretical values of R_{spread} due to the additional local boron doping.

3.3 Recombination at point contacts

To investigate the influence of the laser power on the recombination properties of the point contacts the measured effective lifetime of the samples described in section 2.3 was evaluated using the model proposed by Fischer [8]. This model relates the recombination rate in the passivated area ("S_{pass}") and the metallized area ("S_{met}") considering carrier transport and the spreading resistance of Cox and Strack. This yields the expression for the effective recombination rate S_{eff} of a rear side with local contacts with an area coverage f and D_{min} as the diffusion constant of the minorities

$$S_{eff} = \frac{D_{min}}{W}\cdot\left[\frac{r_c}{2Wf}\arctan\left(\frac{2W}{r_c}\right) - \right. \qquad (2)$$
$$\left. + \exp\left(-\frac{W}{r_c}\sqrt{\frac{f}{\pi}}\right) + \frac{D_{min}}{fWS_{met}}\right]^{-1} + \frac{S_{pass}}{1-f}$$

The results are given in Table I. It is observed that the forming gas anneal is beneficial for the properties of the point contact. The values for S_{met} are in the order of 10^3 cm/s and somewhat lower values are observed for larger contacts at medium to high laser powers. The authors note that the extracted values for S_{met} give an upper boundary for the recombination rate S_{met} as the area of the point contact is determined by light microscopy and possible recombination activity at the edge of the contact is not accounted for.

Table I: Determined values for S_{met} according to expression (2) at the point contacts before and after forming gas annealing (FGA)

Laser power [W]	Point contact diameter [µm]	S_{met} before FGA [cm/s]	S_{met} after FGA [cm/s]
19.5	60	17 500	7 400
13.5	46	29 200	6 500
7.5	26	68 600	13 700

The determined values for S_{met} are lowest for medium laser powers und thus such values are chosen for solar cell processing.

3.4 PERL solar cells

To give proof for the feasibility of this process for LBSF formation for p-type silicon solar cells, a batch of PERC/PERL solar cells have been prepared. Three groups 1 to 3 have been processed, as described in section 2.4. The results of the best cell and mean values for each group are given in Table II.

Table II: Measured *J-V* data for cells of group 1-3. The average value for each group is given as well as the group size (in brackets). The data for the best cell in each group is presented as well.

		η [%]	V_{OC} [mV]	J_{SC} [mA/cm²]	*FF* [%]
PVD PERC	Gr. 1 mean (4)	0.06	288	0.82	25.4
	Gr. 1 best cell	0.09	357	0.97	25.9
PVD B-PERL	Gr. 2 mean (3)	19.6	651	38.2	79.0
	Gr. 2 best cell	20.0	654	38.4	79.4
SP Al-PERL	Gr. 3 mean (5)	19.5	650	38.5	78.2
	Gr. 3 best cell	19.7	651	38.6	78.4

Cells of group 1 (PVD PERC, with no local doping underneath the local contact) perform poorly. These samples exhibit a very high series resistance (R_S > 1 kΩcm²) and it can be concluded that no electrical contact was formed at the rear side between the base and the aluminum. The cell featuring a local boron doping and evaporated rear side Al (Group 2, PVD B-PERL) perform best. Efficiencies up to 20% are achieved at open circuit voltages above 650 mV and fill factors >79%. This good performance is mainly due to the highest fill factors and a higher V_{OC}, highlighting that the proposed process for local boron doping is actually feasible for solar cell production. The high fill factor is due to a low series resistance, as the lateral conductivity of the rear side Al as well as the electrical contact of the local point contacts is excellent. The high open circuit voltage V_{OC} underlines that the cells feature an effective local back surface field.

As the local alloying of screen printed aluminum is currently of interest for industrial application, this approach was also included in Group 3 for comparison: Group 3 (SP Al-PERL) features local Al doping in the contact openings. These cells show a somewhat lower performance in *FF* compared to group 2 (due to higher series resistance R_S). This is attributed to the lower lateral conductivity of the screen printed aluminum as well as the larger line spacing of the rear contact lines. The peak values in V_{OC} are also higher for group 2. This is credited with the lower rear side metal area coverage (point contacts for group 2 with f ~ 1%) compared to group 3 (line contacts with f ~ 3.5%). This is an inherent advantage of the PVD metallization scheme, as no geometrical prerequisites exist for this Al deposition technique as no local Al alloying during fast firing has to be performed and thus the full potential of the boron BSF can be exploited.

4 CONCLUSION

We have presented a novel approach to fabricate local boron doping for p-type silicon PERL solar cells. A boron doped silicon nanoparticle paste is applied onto the passivation layer and can be driven into the wafer by an adapted laser process creating local contact openings at the same time. Sheet resistances R_{sheet} < 30 Ω/sq are observed after laser processing and deep doping up to several microns can be realized. Investigations reveal that these locally doped point contacts allow an excellent ohmic contact with point contact resistances lower than the spreading resistance. P-type PERL solar cells with local boron BSF are fabricated and show efficiencies up to 20.0% on commercial 6-inch MCz-Si.

5 ACKNOWLEDGEMENTS

The authors acknowledge the help of Matthias Weng with the annealing and Dr. Sebastian Mack for discussion of the results.

REFERENCES

1. Blakers, A.W., et al., *22.8% efficient silicon solar cell.* Applied Physics Letters, 1989. **55**(13): p. 1363-5.
2. Zhao, J., A. Wang, and M.A. Green, *24·5% Efficiency silicon PERT cells on MCZ substrates and 24·7% efficiency PERL cells on FZ substrates.* Progress in Photovoltaics: Research and Applications, 1999. **7**(6): p. 471-4.
3. Schneiderlöchner, E., et al., *Laser-fired rear contacts for crystalline silicon solar cells.* Progress in Photovoltaics: Research and Applications, 2002. **10**: p. 29-34.
4. Agostinelli, G., et al. *Local contact structures for industrial perc-type solar cells.* in *Proceedings of the 20th European Photovoltaic Solar Energy Conference*. 2005. Barcelona, Spain.
5. Engelhart, P., et al. *Q.ANTUM - Q-Cells nect generation high-power silicon solar cell & module concept.* in *Proceedings of the 26th European Photovoltaic Solar Energy Conference and Exhibition*. 2011. Hamburg, Germany.
6. Xu, Z., et al. *Industrially rear side passivated Cz mono-crystalline cells with 19.5% efficiency*. in *Proceedings of the 39th IEEE Photovoltaic Specialists Conference*. 2013. Tampa, FL, USA.
7. Tomizawa, Y., Ikeda, Y., Daido, T., Shiro, T. *Laser doping using phosphorous- and boron doped silicon nanoink.* in *28th EU PVSEC.* 2013. Paris.
8. Fischer, B., *Loss analysis of crystalline silicon solar cells using photoconductance and quantum efficiency measurements*, in *Fachbereich Physik*. 2003, Universität Konstanz: Konstanz. p. 198.
9. Cox, R.H. and H. Strack, *Ohmic contacts for GaAs devices.* Solid State Electronics, 1967. **10**: p. 1213-8.